

Somatic *TARDBP* variants as a cause of semantic dementia

 Jeroen van Rooij,^{1,2}  Merel O. Mol,¹ Shamiram Melhem,¹ Pelle van der Wal,² Pascal Arp,² Francesca Paron,³ Laura Donker Kaat,^{1,4}  Harro Seelaar,¹ Netherlands Brain Bank, Suzanne S. M. Miedema,⁵ Takuya Oshima,⁶ Bart J. L. Eggen,⁶ André Uitterlinden,² Joyce van Meurs,² Ronald E. van Kesteren,⁵ August B. Smit,⁵  Emanuele Buratti³ and John C. van Swieten¹

The aetiology of late-onset neurodegenerative diseases is largely unknown. Here we investigated whether *de novo* somatic variants for semantic dementia can be detected, thereby arguing for a more general role of somatic variants in neurodegenerative disease. Semantic dementia is characterized by a non-familial occurrence, early onset (<65 years), focal temporal atrophy and TDP-43 pathology. To test whether somatic variants in neural progenitor cells during brain development might lead to semantic dementia, we compared deep exome sequencing data of DNA derived from brain and blood of 16 semantic dementia cases. Somatic variants observed in brain tissue and absent in blood were validated using amplicon sequencing and digital PCR. We identified two variants in exon one of the *TARDBP* gene (L41F and R42H) at low level (1–3%) in cortical regions and in dentate gyrus in two semantic dementia brains, respectively. The pathogenicity of both variants is supported by demonstrating impaired splicing regulation of TDP-43 and by altered subcellular localization of the mutant TDP-43 protein. These findings indicate that somatic variants may cause semantic dementia as a non-hereditary neurodegenerative disease, which might be exemplary for other late-onset neurodegenerative disorders.

- 1 Department of Neurology, Erasmus Medical Center, Rotterdam, The Netherlands
- 2 Department of Internal Medicine, Erasmus Medical Center, Rotterdam, The Netherlands
- 3 International Centre for Genetic Engineering and Biotechnology (ICGEB), Trieste, Italy
- 4 Department of Clinical Genetics, Erasmus Medical Center, Rotterdam, The Netherlands
- 5 Center for Neurogenomics and Cognitive Research, VU University, Amsterdam, The Netherlands
- 6 Department of Biomedical Sciences of Cells and Systems, section Molecular Neurobiology, University of Groningen, University Medical Center Groningen (UMCG), Groningen, The Netherlands

Correspondence to: Prof. John van Swieten, MD
Erasmus Medical Center, Dr. Molewaterplein 40, 3015GD, Rotterdam, The Netherlands
E-mail: j.c.vanswieten@erasmusmc.nl

Keywords: semantic dementia; somatic variants; *TARDBP*; TDP-43

Abbreviation: FTD = frontotemporal dementia

Introduction

Multifactorial aetiology, including genetic and environmental factors, has been used to explain most late-onset neurodegenerative diseases. Only a small percentage of cases with

autosomal dominant inheritance is caused by germline variants in specific genes, for example *PSEN1* and *APP* variants in Alzheimer's disease, *MAPT* and *GRN* in frontotemporal dementia (FTD) and *C9orf72* and *TARDBP* in both

Received April 17, 2020. Revised July 13, 2020. Accepted August 06, 2020. Advance access publication November 6, 2020

© The Author(s) (2020). Published by Oxford University Press on behalf of the Guarantors of Brain.

This is an Open Access article distributed under the terms of the Creative Commons Attribution Non-Commercial License (<http://creativecommons.org/licenses/by-nc/4.0/>), which permits non-commercial re-use, distribution, and reproduction in any medium, provided the original work is properly cited. For commercial re-use, please contact journals.permissions@oup.com

amyotrophic lateral sclerosis and FTD (Ferrari *et al.*, 2019; Greaves and Rohrer, 2019; Clarimon *et al.*, 2020). There is an increasing interest in the potential pathogenic role of *de novo* variants in patients with neurodegenerative diseases with a negative family history (Leija-Salazar *et al.*, 2018; Lodato and Walsh, 2019). A few cases with *de novo* germline variants have been identified in early-onset Alzheimer's disease (Nicolas *et al.*, 2018). For neurodevelopmental diseases, low-level ($\leq 20\%$ of cells) somatic variants in *mTOR*, *AKT3* and *CCND* arising from the ventricular or subventricular zone have been identified by deep sequencing of candidate genes in affected brain tissue (Lee *et al.*, 2012; Lin *et al.*, 2012; Veltman and Brunner, 2012; Miller *et al.*, 2013; Poduri *et al.*, 2013; Hu *et al.*, 2014; Jamuar *et al.*, 2014; Kovacs *et al.*, 2014; Mirzaa *et al.*, 2014; Rogalski *et al.*, 2014; Bushman *et al.*, 2015; Lim *et al.*, 2015; Lodato *et al.*, 2015; Sala Frigerio *et al.*, 2015; Wiseman *et al.*, 2015; Hoekstra *et al.*, 2016; Kim *et al.*, 2016; Takata *et al.*, 2016). The hypothesis is that post-zygotic variants (after fertilization) or late-somatic variants during brain development might explain the sporadic presentation of neurodegenerative diseases with a negative family history.

The most ideal approach to determine the role of late-somatic variants in neurodegenerative diseases would be the comparison between blood- and brain-derived DNA within the same patients. However, brain tissue for DNA isolation was often not available during life, and DNA derived from blood was often not collected during life in deceased patients. Recent brain-derived DNA studies without matched DNA samples from blood have tried to detect somatic variants in Alzheimer's and Parkinson's disease (Beck *et al.*, 2004; Lin *et al.*, 2012; Proukakis *et al.*, 2014; Bushman *et al.*, 2015; Lodato *et al.*, 2015; Sala Frigerio *et al.*, 2015; Wiseman *et al.*, 2015; Coxhead *et al.*, 2016; Hoekstra *et al.*, 2016; Lee *et al.*, 2018; Lodato *et al.*, 2018; Mokretar *et al.*, 2018; Nicolas *et al.*, 2018; Park *et al.*, 2019; Wei *et al.*, 2019). A higher number of low-level mosaic variants in causative genes (*APP*, *SNCA*) have been detected in DNA of Alzheimer's disease or Parkinson's disease brains compared to controls (Lee *et al.*, 2018; Mokretar *et al.*, 2018). Only the study by Park *et al.* (2019) performing deep sequencing of hippocampal formation and matched blood tissues found an enrichment of somatic DNA variation in the Tau signaling pathway in Alzheimer's disease patients compared to controls (Park *et al.*, 2019). Specifically, a single carrier of a somatic variant in *PIN1* was suggested as potential causal factor in the respective Alzheimer's disease patient (Park *et al.*, 2019).

In the present study, we uniquely investigated the presence of low-level somatic variants in the temporal cortex and dentate gyrus of brains of patients with semantic dementia, which were absent in their blood-derived DNA. Semantic dementia is a well-defined clinical and pathological subtype of FTD, mostly occurring before the age of 65 (Hodges *et al.*, 1992; Irish *et al.*, 2012; Mesulam *et al.*, 2014). The disease is characterized by a circumscribed asymmetric atrophy of the anterior temporal cortex, suggesting a local disease

process (Mummery *et al.*, 2000; Kumfor *et al.*, 2016). Severe neuronal loss with pathological TDP-43 protein accumulation in neurites and neurons in the temporal cortex and dentate gyrus of the hippocampus are the defining salient and consistent neuropathological features of semantic dementia, most commonly classified as FTD-TDP type C (Davies *et al.*, 2005; Mackenzie *et al.*, 2011; Leyton *et al.*, 2016; Neumann and Mackenzie, 2019). Semantic dementia has a sporadic, non-familial occurrence, and a current lack of mechanistic insight in the disease process precludes a therapeutic strategy. We performed deep exome sequencing ($310\times-658\times$) of middle temporal gyrus and dentate gyrus tissue of semantic dementia patients with pathologically confirmed FTD-TDP type C, and compared data with blood DNA samples of the same patients. We identified somatic *TARDBP* variants in the brains of two semantic dementia patients that were absent in blood. These variants were validated using custom amplicon panel sequencing and digital droplet PCR. In addition, we confirmed the disruptive effects of these *TARDBP* variants by demonstrating altered cellular distribution of the mutant TDP-43 proteins. Our results indicate that somatic variants in *TARDBP* contribute to semantic dementia pathogenesis.

Materials and methods

Patient tissue DNA collection

For the present study, we used fresh-frozen brain samples from 16 semantic dementia patients with confirmed FTD-TDP type C pathology, obtained from the Netherlands Brain Bank (Table 1) (Mackenzie and Neumann, 2017). Informed consent was obtained from all patients for brain autopsy and the use of tissue and clinical information for research purposes. DNA was extracted from fresh frozen brain samples of middle temporal gyrus ($n = 14$) and from the dentate gyrus ($n = 13$). From all cases, DNA from blood was available, obtained during life in 12 patients from the Dutch FTD study and extracted from blood obtained at the time of autopsy in the remaining four cases (Seelaar *et al.*, 2008, 2011). The average age at death was 69 (range 62–74), 50% of patients were female. Medical records and neuroimaging (either CT or MRI) were collected and reviewed, if available. For 14 patients the left hemisphere of the brain was fresh-frozen for research, versus the right hemisphere for two patients.

Whole exome sequencing

Blood-derived DNA of 16 patients and brain-derived DNA from middle temporal gyrus ($n = 14$) and/or dentate gyrus ($n = 13$) of semantic dementia brains ($n = 16$) was captured using Nimblegen's SeqCap or MedExome library prep kits and sequenced to an average depth of $139\times$, $496\times$ and $395\times$, respectively. Reads were mapped to the hg19 reference genome using BWA and processed using picard and GATK, following best practices. Candidate variants were called using thresholds to detect variants present in the brain (> 5 reads), but absent in blood (≤ 1 read). The next three filtering steps for candidate

variants were; (i) a custom signal to noise filter ($S2N \geq 5$) as described in the [Supplementary material](#); (ii) a minor allele frequency $< 0.01\%$ in the ExAC database; and (iii) a CADD score above 10.

Validation amplicon panel sequencing

We validated a selection of candidate variants (present in brain, absent in blood) to confirm true-positive variants, and two candidate genes (*GRN* and *TARDBP*) to exclude false negatives, by amplicon panel sequencing of the same DNA samples used in the discovery whole exome sequencing. All candidate variants in these targets were included in a custom amplicon panel (SWIFT, product code SW CP-ER6161) and sequenced to an average depth of $1601\times$ on a MiSeq v3 with 600 cycles. A second round of amplicon panel sequencing was carried out for further classification of somatic variants of interest in DNA from additional cortex regions (middle frontal gyrus, superior parietal lobe) and cerebellum of two semantic dementia brains, and in DNA from middle temporal gyrus of 66 non-demented control brains from the Netherlands Brain Bank. Data analysis of the panel was done similar to the discovery. Candidate somatic variants were validated when: (i) read depth in the validation was at least 100; (ii) the variant allele count was at least 20 in DNA of the brain; (iii) the variant allele frequency was at least 1% in DNA of the brain; and (iv) variant allele frequency was $< 1\%$ in blood of the same patient.

Validation of *TARDBP* variants

We performed additional validation using digital droplet PCR of two *TARDBP* somatic variant carriers. In short, custom LNA FAM+HEX probes for each variant were designed and

optimized by TATAA Biocenter. Synthetic DNA fragments (gBlocksTM) with these variants were generated to serve as positive controls and as a dilution ladder for technical evaluation of the assay. Negative controls were water and DNA of middle temporal gyrus from two unrelated non-demented controls. Each assay was tested on five brain regions of the carrier (medial temporal gyrus, medial frontal gyrus, superior parietal gyrus, dentate gyrus and cerebellum), blood and the two negative controls. Droplets were generated using Bio-Rad's Droplet Generation Oil for Probes (cat#1863005) in combination with the qPCR Droplet PCR supermix (no dUTP, Bio-Rad cat#1863024) on a Bio-Rad QX200 Droplet Generator. The PCR plate was measured using the QX200 Droplet Reader (Bio-Rad) and analysed with the Quantasoft Analysis Pro software (Bio-Rad). Reactions with fewer than 10 000 accepted droplets were not used in the analysis. Sensitivity rates of the assays were established using 0.1%, 1.0% and 2.5% spiked positive control gBlocksTM mutation fragments and subsequently used to estimate variant allele frequencies by the ratio of FAM-positive droplets over HEX-positive droplets.

Germline variants in blood and brain

To exclude (*de novo*) germline variants in 12 FTD (*CHMP2B*, *DPP6*, *FUS*, *GRN*, *MAPT*, *OPTN*, *SQSTM1*, *TARDBP*, *TBK1*, *TREM2*, *UNC13A* and *VCP*) candidate genes we performed regular germline variant calling using GATK's Haplotypecaller using best practices ([van Rooij et al., 2017](#); [Ferrari et al., 2019](#); [Greaves and Rohrer, 2019](#); [Clarimon et al., 2020](#)). Variants were annotated using annovar and were manually evaluated based on exonic function, CADD score, frequency in GnomAD, variant allele frequency and presence in the other tissues of the same patient.

Table 1 Patient characteristics

Patient	Sex	Age at onset	Disease duration	Dominant side pathology	Brain tissue side	Dominant side	MTG	DG
SD01	Female	60	10	Both	Left	No	Yes	No
SD02	Male	48	14	Left	Left	Yes	No	Yes
SD03	Female	60	8	Both	Left	NA	Yes	No
SD04	Female	45	20	Both	Left	NA	Yes	Yes
SD05	Male	56	10	Both	Left	No	Yes	Yes
SD06	Male	51	12	Both	Left	No	Yes	Yes
SD07	Female	53	11	Both	Left	No	No	Yes
SD08	Male	57	12	Left	Left	Yes	Yes	Yes
SD09	Female	63	11	Both	Left	NA	Yes	Yes
SD10	Male	55	13	Left	Right	No	Yes	Yes
SD11	Male	51	15	Both	Left	No	Yes	Yes
SD12	Female	60	12	Both	Left	No	Yes	Yes
SD13	Female	63	9	Left	Right	No	Yes	Yes
SD14	Male	57	15	Both	Left	No	Yes	Yes
SD15	Female	66	8	Left	Left	Yes	Yes	No
SD16	Male	61	13	Both	Left	Yes	Yes	Yes

Contains clinical and pathological information on the patients examined in this study. Pathological diagnosis, as extracted from the reports from the Netherlands Brain Bank. The most affected side of the brain is reported according to the post-mortem pathological examination. Brain tissue side: the side of the brain fresh frozen and used in this study. Dominant side yes/no; whether the side studied was the one most affected according to neuroimaging (NA = not applicable, as both sides were equally affected). Middle temporal gyrus (MTG) and dentate gyrus (DG) indicate whether these areas were available and included in the study.

Functional analysis of somatic *TARDBP* variants

The functional impact of both somatic *TARDBP* variants on the TDP-43 protein was assessed by a previously published add-back splicing assay and by immunofluorescent microscopy of TDP-43 in HeLa cells (D'Ambrogio *et al.*, 2009). In short, the splicing assay contains a minigene construct containing *CFTR* exon 9 carrying a mutation (C155T) in an exonic splicing enhancer sequence in order to have a ~50% chance of in- or out-splicing of exon 9. Using wild-type TDP-43 as positive control, and complete loss-of-function F4L mutated TDP-43 as negative control, the relative impact of L41F and R42H on TDP-43 function could be ascertained. To obtain *P*-values, an unpaired *t*-test was carried out using GraphPad software (GraphPad Software, La Jolla California, USA). For the immunofluorescence assays, HeLa cells were transfected with wild-type TDP-43 or with TDP-43 carrying variants L41F or R42H. Nuclei were located by chromatic staining of DAPI, and co-localization of TDP-43 is identified by FLAG-TDP-43 protein, as published previously (Mompean *et al.*, 2017). FLAG TDP-43 staining was quantified using regions of interest for nuclear and cytoplasmic signal using Fiji ImageJ software. The percentage of nuclear and cytoplasmic fluorescent signal was measured for nine cells each for the wild-type, L41F and R42H TDP-43 expressing cells. Statistical tests were performed using two-way ANOVA in GraphPad for nuclear-cytoplasmic TDP-43 localization within each cell-line, as well as between the wild-type and the L41F or R42H TDP-43 transfected cells.

Cell-type specificity of the somatic R42H *TARDBP* variant

For the R42H *TARDBP* variant carrier, we performed fluorescence-activated nuclear sorting (FANS) on the frontal lobe and parietal lobe, then isolated DNA from the nuclei with QIAamp DNA Micro Kit (QIAGEN). Using NeuN and Olig2 as cell surface markers, we separated neurons (NeuN-positive) and oligodendrocytes (Olig2-positive) from microglia, astrocytes and any other nuclei (double negative). Parietal cortex tissue from a dementia patient unrelated to this study was similarly sorted and used as negative control. Each resulting DNA sample was amplicon sequenced and analysed using the described procedures.

Data availability

All main results are available through Tables 1, 2 and Supplementary Tables 1–3. Additional data from the raw results are available on request from the authors.

Results

Deep whole exome sequencing

All DNA samples from middle temporal gyrus ($n = 14$), dentate gyrus ($n = 13$) and blood ($n = 16$) were sequenced to an average depth of 496 (range 429–658), 395 (range 310–520) and 139 (range 72–229), respectively.

Exclusion of causal germline variants

Germline variant analysis in the whole exome sequencing data of all semantic dementia patients did not result in known pathogenic variants in any of the 12 known FTD genes. One patient was identified as germline carrier of the V90A variant in *TARDBP*, which was also reported in controls and thus considered of uncertain significance (Supplementary Table 1) (Borroni *et al.*, 2010; Lattante *et al.*, 2013; Caroppo *et al.*, 2016).

Discovery and validation of somatic variants in semantic dementia brains

After signal to noise, minor allele frequency and CADD score filtering we retained on average 172 variants for dentate gyrus and 57 for middle temporal gyrus per patient (Fig. 1 and Supplementary Fig. 1). We detected variants in 1450 genes from the dentate gyrus and/or middle temporal gyrus of at least one semantic dementia patient and absent in blood. To confirm true-positive variants, we selected a set of 305 variants for validation in a panel of amplicon sequencing based on one of the two following criteria: (i) somatic variants present in at least five brains (resulting in 252 variants in a total of 128 genes); or (ii) variants in candidate genes involved in neurodevelopmental or neurodegenerative diseases (resulting in 53 variants in 51 genes present in one to four brains). Amongst the 51 candidate genes fulfilling the second criterion were single variant carriers in *TARDBP* (R42H) and in *GRN*.

We identified eight true-positive variants in the panel of amplicon sequencing ($\geq 100 \times$ depth in both brain and blood, variant observed ≥ 20 times in the brain, variant allele frequency of $\geq 1\%$ in brain and $\leq 1\%$ in blood). Seven of those were previously detected with exome sequencing, whereas the eighth variant was not detected in exome sequencing but identified through rescreening of the *TARDBP* gene in the amplicon sequencing data (Table 2). The non-synonymous variant (R42H) in *TARDBP*; chr1:11073909-G/A with a CADD score of 20 was the most significantly replicated variant (271 of 18 990 sequenced fragments in middle temporal gyrus, and none of 5126 fragments in blood) and completely absent from gnomAD (variant allele frequency of 1.4% in the middle temporal gyrus of a single semantic dementia brain).

A second non-synonymous variant in the same exon; chr1:11073905-C/T (L41F) in the *TARDBP* gene was detected in the dentate gyrus of another patient with variant allele frequency of 2.0% in the amplicon panel sequencing data [152 of 7533 fragments, $P = 2.8 \times 10^{-47}$, odds ratio (OR) = 47, 95% confidence interval (CI) = 18–175, compared to blood]. This variant with a CADD score of 28 was also absent from the population databases, and was not observed in blood-derived DNA or any of other brain

Table 2 Summary of results of eight validated somatic variants

Variant	Gene	Function	Sample	Tissue	S2N	MAF	CADD	WES-Blood			WES-Brain			Panel-Blood			Panel-Brain			P-value	
								REF	ALT	VAF	REF	ALT	VAF	REF	ALT	VAF	REF	ALT	VAF		
chr1:11073909:G/A	TARDBP	Nonsyn	SD14	MTG	9.8	0	20	87	0	0.000	765	10	0.013	0.6	5126	0	0.000	18719	271	0.014	9×10^{-29}
chr1:11073909:C/T	TARDBP	Nonsyn	SD10	DG	NA	0	28	138	0	0.000	1037	0	0.000	1	9349	4	0.000	7533	152	0.020	3×10^{-47}
chr9:130928555:T/G	CIZ1	Nonsyn	SD11	DG	20.8	0	16	39	0	0.000	323	54	0.143	0.005	134	0	0.000	346	35	0.092	3×10^{-5}
chr17:4883215:A/G	CAMTA2	Nonsyn	SD09	DG	11.1	0	18	58	1	0.017	420	42	0.091	0.07	146	1	0.007	1058	24	0.022	0.4
chr17:3419231:T/G	HEATR9	Nonsyn	SD11	DG	7.6	0	13	72	0	0.000	278	21	0.070	0.02	3232	24	0.007	18031	329	0.018	3×10^{-6}
chr17:70119726:C/A	SOX9	Nonsyn	SD14	DG	9.0	0	20	56	1	0.018	405	15	0.036	0.7	1676	5	0.003	1133	76	0.063	9×10^{-24}
chr19:51133405:A/G	SYT3	Nonsyn	SD11	DG	8.5	0	14	14	0	0.000	227	25	0.099	0.4	103	0	0.000	1593	29	0.018	0.4
chr19:51133405:A/G	SYT3	Nonsyn	SD09	DG	12.4	0	14	21	0	0.000	236	40	0.145	0.09	289	1	0.003	1829	29	0.016	0.2

All eight variants passed the validation criteria. WES-Blood/WES-Brain shows the read counts for variant and wild-type from exome sequencing. Panel-Blood/Panel-Brain shows the counts for the amplicon panel. ALT = number of reads carrying the alternative allele; MAF = minor allele frequency; Nonsyn = non-synonymous; REF = number of reads carrying the reference allele; S2N = signal to noise; VAF = variant allele frequency. P-values were obtained by Fisher's exact tests of the counts between blood and brain.

regions of the same patient (Fig. 2). Both variants observed in a single patient each were taken forward for further validation by digital PCR and functional testing, as germline variants in *TARDBP* are known to cause FTD and/or amyotrophic lateral sclerosis with TDP-43 pathology (Borroni *et al.*, 2010; Lattante *et al.*, 2013; Caroppo *et al.*, 2016).

Validation of *TARDBP* variant R42H by amplicon sequencing, digital droplet PCR

After confirming presence of this variant in middle temporal gyrus (271 fragments of 18 990, $P = 8.9 \times 10^{-29}$) and absence in 5123 sequenced fragments from blood, we validated this variant in other cortical regions of the same brain. We observed this variant with similar frequency in the parietal lobe (1.2%, 12 of 973 fragments, $P = 2.3 \times 10^{-10}$), in the frontal lobe (0.5%, 11 of 2,122 fragments, $P = 1.3 \times 10^{-6}$), and at lower frequency in the hippocampus (0.3%, 8 of 3021 fragments, $P = 3.6 \times 10^{-4}$) and cerebellum (0.1%, 3 of 2881 fragments, $P = 4.7 \times 10^{-2}$), although the variant allele frequency observed in hippocampus and cerebellum were within the range observed in the other samples, as shown in Fig. 2A. The variant was not observed among temporal cortex samples of 66 non-demented controls (0.03%, total 28 fragments of 106 635, likely representing random sequencing errors). The R42H variant was then sequenced in only neuronal nuclei (NeuN-positive), oligodendrocyte nuclei (Olig2-positive) or the nuclear fraction containing, amongst others, astrocytes and microglia (and other NeuN/Olig2 double negative CNS cell nuclei) in both frontal and parietal lobe of the R42H carrier to an average depth of $3579 \times$. The R42H variant was detected in 2.4% of the neurons in the parietal lobe and 1.1% in the frontal lobe (74 and 42 fragments of 3093 and 3806 in total, respectively). These frequencies were doubled compared the bulk parietal and frontal tissue (1.2% and 0.5%, respectively). The variant was not observed in the control sample ($<0.1\%$) and at three to four times lower frequencies in the oligodendrocytes or double negative nuclear fraction ($<0.5\%$ in the parietal lobe and $<0.4\%$ in the frontal lobe, respectively).

Validation using digital droplet PCR confirmed the amplicon sequencing results, as shown by the allelic discrimination plots (Fig. 3). The variant was observed in 242 droplets of 13 048 non-empty droplets (variant allele frequency = 1.9%) in the temporal lobe which was significantly higher than the negative controls; blood of the same patient (variant allele frequency = 0.1%, 1 of 809 droplets, $P = 1.1 \times 10^{-5}$) and temporal lobe of two non-demented controls (variant allele frequency = 0.04%, 3 of 7698 droplets, $P = 1.5 \times 10^{-44}$). Similarly, the variant was observed at significantly higher levels compared to the controls in the frontal lobe (variant allele frequency = 1.3%, 126 droplets of 9549, $P = 6.7 \times 10^{-4}$ and $P = 1.1 \times 10^{-28}$) and parietal lobe (variant allele frequency = 0.6%, 21 of 3697 droplets,

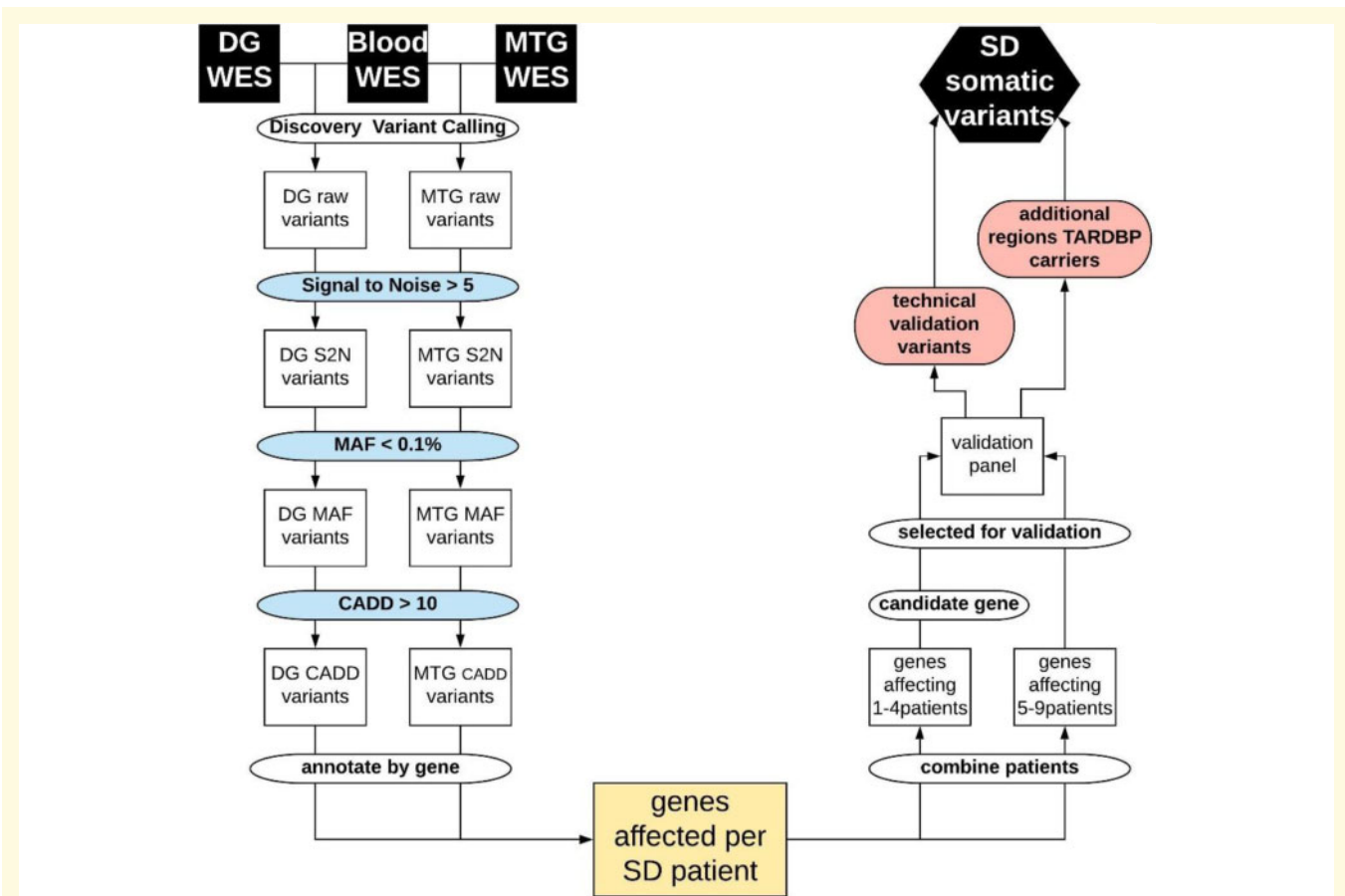


Figure 1 Flowchart of data filtering and analysis. From top left: Raw somatic variant calling using blood and dentate gyrus (DG) or medial temporal gyrus (MTG) deep exome sequencing data (WES), signal to noise filter (S2N), minor allele frequency filter (MAF), CADD score filter, annotating and grouping per gene, resulting in the genes affected in each patient with semantic dementia (SD). Right: Grouping genes affecting multiple patients (>5) or affecting candidate genes in fewer patients (one to four) to be included in the validation amplicon panel. To excluded false negative findings in the WES data in FTD-TDP known germline causal genes *GRN* and *TARDBP*, all exons in these genes were included in the validation panel. The first validation round was performed on the same tissues as the discovery WES to confirm true positive variants from the WES, or identify false negative findings in *GRN* or *TARDBP*. The second round of validation further classified true positive variants in additional brain tissues and non-demented controls.

$P = 0.16$ and $P = 3.5 \times 10^{-8}$) and cerebellum (variant allele frequency = 0.1%, 13 of 9231 droplets $P = 1.0$ and $P = 0.04$).

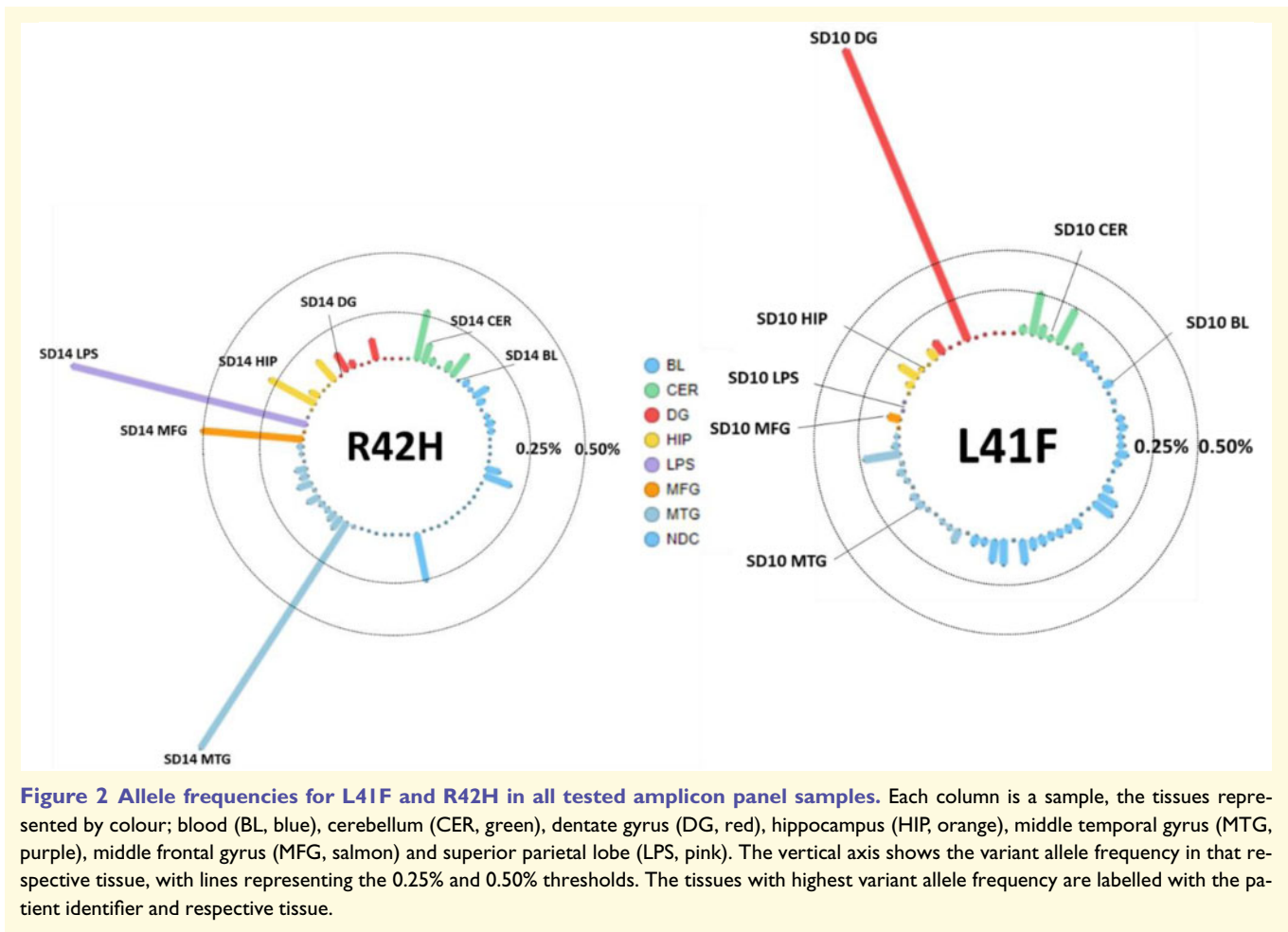
Validation of *TARDBP* variant L41F by amplicon sequencing, digital droplet PCR

The second *TARDBP* somatic variant in the same exon was detected in the dentate gyrus with a variant allele frequency of 2.0% in the amplicon panel sequencing data (152 of 7533 fragments, $P = 2.8 \times 10^{-47}$) compared to blood (Fig. 2B). The variant was not observed among temporal cortex samples of 66 non-demented controls (0.04%, total 39 fragments of 106 632, likely representing random sequencing errors). Validation with digital droplet PCR confirmed absence of the variant in blood, cerebellum, frontal lobe, temporal lobe and parietal lobe. Because of the low quantity of DNA from laser-capture microdissection-derived

dentate gyrus, this tissue could not be tested using digital PCR. This may have also influenced the whole exome sequencing (WES) result, in which many PCR duplicates were observed for the dentate gyrus data. We did not find any other somatic variants in the *TARDBP* gene in any of the other semantic dementia brains (average coverage across the gene of 1116) and also not in middle temporal gyrus of non-demented control samples (average coverage of $103 \times$ across the gene).

Clinicopathological description of the two cases with somatic *TARDBP* variants

Both patients carrying the *TARDBP* L41F or R42H somatic variant developed progressive problems with word finding and language comprehension, and visual agnosia at the age of 55 and 57, respectively. Compulsive-obsessive behaviour, loss of initiative and emotional lability were salient features



in both patients, similar to the other 14 patients. Profound left-sided temporal atrophy was observed by neuroimaging (CT, MRI) 2 and 3 years after onset in both *TARDBP* carriers, in contrast to asymmetric but bilateral atrophy in the other semantic dementia patients (Fig. 4). Neuropathological examination after death (68 and 72 years, respectively) showed severe anterior temporal atrophy, left more pronounced than right in the L41F carrier and more symmetrical in R42H. Microscopically, neuropathological changes were consistent with TDP-pathology type C, with severe neuron loss, gliosis in the temporal cortex with long thick threads and round cytoplasmic inclusions in granular cells of the hippocampus. For the L41F carrier, DNA of the middle temporal gyrus from the right hemisphere was available in the Netherlands Brain Bank and used for all DNA analyses, for the carrier of the R42H variant this was the middle temporal gyrus of the left hemisphere.

Functional analysis of *TARDBP* variants

TDP-43 (encoded by *TARDBP*) is a protein involved in RNA splicing (Buratti and Baralle, 2001; D'Ambrogio *et al.*, 2009). Therefore, the impact of both *TARDBP* variants on

the activity and localization TDP-43 was established in two assays; splicing regulation and cellular localization. The splicing assay contains a minigene construct containing *CFTR* exon 9 carrying a mutation (C155T) in an exonic splicing enhancer sequence in order to have ~50% chance of in- or out-splicing of exon 9. The splicing is mediated by TDP-43 binding to the UG-repeat sequences near the 3' start site. Thus, when the function of TDP-43 is lost upon targeted small interfering RNA (siRNA) treatment, a decrease to ~20% of exon 9 skipping is observed. Exon 9 skipping is then rescued by adding back wild-type TDP-43 whose transcript has been made resistant to siRNA treatment. As negative control, we used a construct containing a TDP-43 that carries variant F4L, which is also resistant to the siRNA treatment but cannot bind RNA (Buratti and Baralle, 2001). In the presence of these positive and negative controls, the impact of uncharacterized TDP-43 variants can then be evaluated by comparing the amount of exon 9 skipping of each expressed variant. Both variants significantly decreased exon 9 skipping compared to wild-type TDP-43, as shown in Fig. 5. Splicing impairment was stronger for the L41F variant than for the R42H variant, in accordance with the predicted impact with CADD scores of 28 and 20, respectively. The impact on TDP-43 function was smaller for both

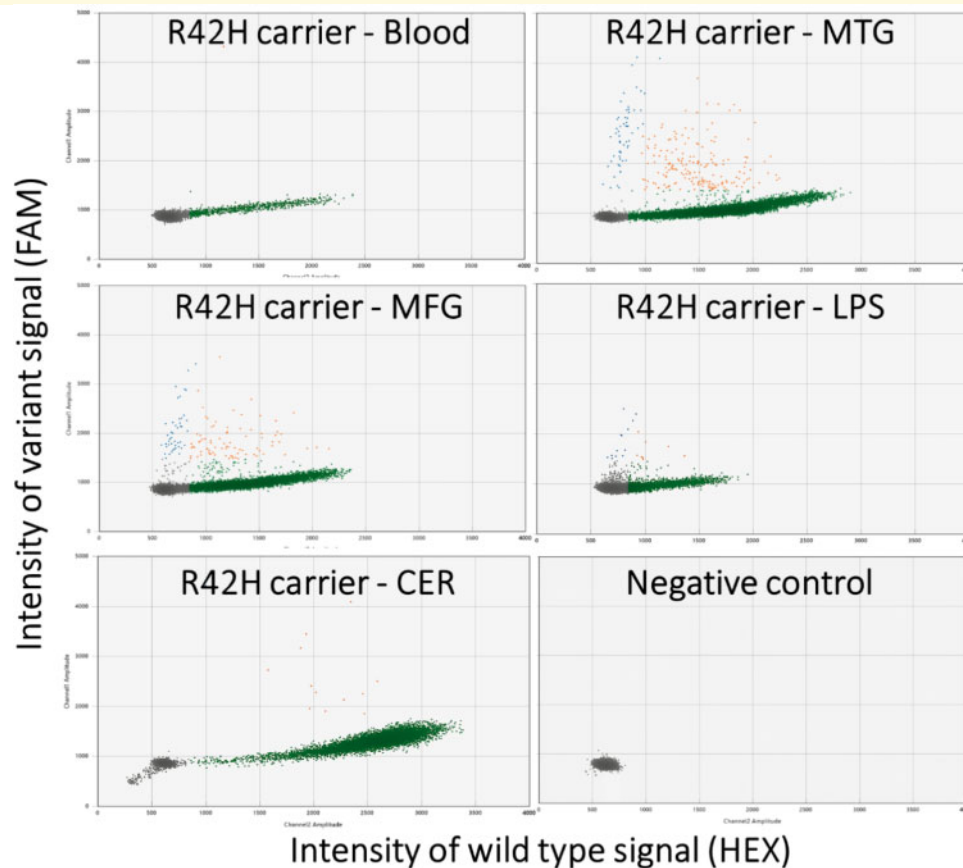


Figure 3 Allelic discrimination plots of the digital droplet PCR for the R42H *TARDBP* somatic variant. Each marker represents a single droplet and its respective wild-type (horizontal axis) and variant (vertical axis) signal intensity. Five different tissues of the carrier were tested: blood, middle temporal gyrus (MTG), middle frontal gyrus (MFG), lateral parietal lobe (LPS), cerebellum (CER) and a negative control of water is shown. The grey droplets are considered empty, green droplets are wild-type only, orange is both wild-type and variant alleles, and blue droplets were harbouring only the variant allele.

variants compared to the siRNA-resistant TDP-43 variant F4L, which blocks RNA binding completely. Immunofluorescent staining demonstrated significantly altered localization of the R42H mutant TDP-43 protein compared to wild-type TDP-43 (Fig. 6). In the wild-type cells, 78% of the fluorescent signal was nuclear ($n = 9$), versus 71% for the L41F cells ($P = 0.54$) and 52% for the R42H cells ($P = 0.0004$). Only in the R42H TDP-43 expressing cells was TDP-43 no longer significantly localized in nuclei compared to cytoplasm. Region of interest measurements and statistical results are provided in Supplementary Table 2.

Discussion

The present study identified the occurrence of two low-level pathogenic somatic variants in the *TARDBP* gene in brains of patients with semantic dementia. These two variants in the first exon of the gene are absent from public databases and significantly affect TDP-43 function and localization. Moreover, the temporal lobe atrophy observed by MRI

neuroimaging 3 years after onset in one of the two somatic *TARDBP* variant carriers resembled classical FTD due to germline *TARDBP* variants.

The observed low level (1–3%) of *TARDBP* somatic variants in brain-derived DNA was in accordance with the hypothesis that somatic variants occurred in one or more clones of neurons acquired in a single neural progenitor cells during brain development. Subsequently, the pathophysiological process arising from neurons carrying the somatic variants would then result in focal neurodegeneration later in life. The low percentage may further be attributed to by selective loss of neurons that carried the somatic variants in the affected brain region. The presence of somatic variants shared by (a) clone(s) of neurons in the temporal cortex or dentate gyrus was in contrast to recent studies, which investigated post-mitotic somatic mosaicism (pathogenic single-nucleotide variants and somatic copy-number variations) of known germline disease genes in individual cells (Lee et al., 2018; Lodato et al., 2018; Mokretar et al., 2018). Such post-mitotic somatic variants increased with age in the latter studies and were found in significantly higher number in

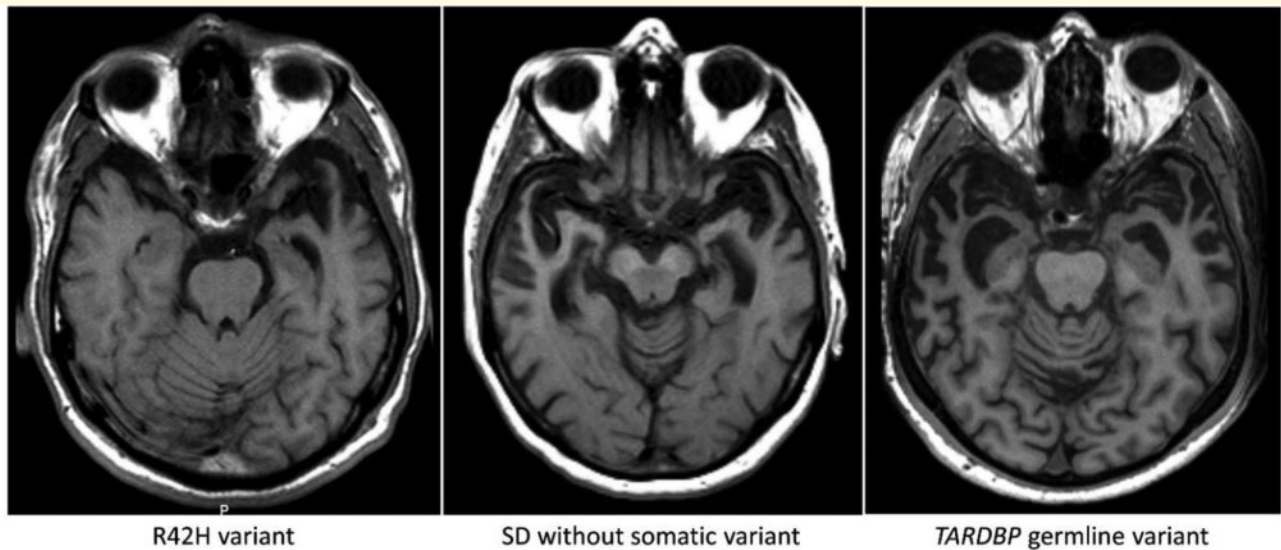


Figure 4 Axial T₁-weighted MRI of the semantic dementia patient carrying somatic variant R42H, showing profound left-sided temporal atrophy 3 years after disease onset. Pathological examination 15 years after disease onset showed atrophy of both temporal poles. The *middle* image is from a patient without a somatic variant (4 years after onset) showing atrophy of both temporal lobes. *Right*: A patient with the germline (p.I383V) *TARDBP* variant, showing a similar atrophy pattern bilaterally (4 years after onset).

Alzheimer's disease or Parkinson's disease brains compared to controls (Lee *et al.*, 2018; Lodato *et al.*, 2018; Mokretar *et al.*, 2018). Although these somatic DNA variations for age-associated brain diseases were potential interesting, their causal role could not be determined for sure (Lodato *et al.*, 2018).

Post-mitotic variants are a less likely cause for semantic dementia in patients as the disease occurs at a relatively young onset age (<65 years) and its prevalence does not increase with age (Hodges *et al.*, 2010; Landin-Romero *et al.*, 2016). Therefore, our sequencing of DNA from bulk tissue, aiming to identify variants shared by neurons, and estimating their variant-allele-frequencies resembled the study of Park *et al.* (2019) in which somatic variants were found per brain region (hippocampal formation) in both Alzheimer's disease patients and controls.

The presence of single somatic variants (R42H and L41F) in the *TARDBP* gene in several neocortical regions (temporal, frontal and parietal) or dentate gyrus strongly points to the initial occurrence of somatic mosaicism in a single neural progenitor cell (Zilles *et al.*, 2013; Palomero-Gallagher and Zilles, 2019). Somatic variants in neurons arising from the ventricular or subventricular zone have also been shown in childhood or adult neurological diseases (Lee *et al.*, 2012; Lim *et al.*, 2015). By using blood-derived DNA from the same patients as control tissue, we could exclude somatic variants occurring from non-ectodermal lineages (Leija-Salazar *et al.*, 2018). Somatic *TARDBP* variants could be excluded from 66 non-demented controls by using temporal cortex-derived DNA. As the specific somatic variant (R42H) was absent in both hippocampus and cerebellum of the same patient, the variant must have occurred in neural

progenitor cells of the lateral segment of the pallium, which develops into the neocortex (Zilles *et al.*, 2013; Palomero-Gallagher and Zilles, 2019). The variant was enriched (twice as frequent compared to bulk cells) in the neuronal subpopulation of the parietal and frontal lobes, further suggesting the neural origin. A low signal (<20% of signal in the neuronal fraction) of the variant in the other nuclear fractions is a likely due to some residual neuronal nuclei present in the NeuN-negative fraction. Based on these results, we estimate that the R42H variant is present in 5.6%, 4.8% and 2.2% of the neurons in the temporal, parietal and frontal lobes, respectively. The second variant (L41F) was only detected in the hippocampus, suggesting that it occurred in neural progenitor cells of the medial segment of the pallium. The asymmetric onset of the disease pathology in these cases did not necessarily require the occurrence of the somatic variants after developmental separation of both hemispheres, as germline variants have also been associated with other asymmetric neurodegenerative disease processes (Stiles and Jernigan, 2010; Caroppo *et al.*, 2016; Gonzalez-Sanchez *et al.*, 2018). Although of interest, due to the collection procedure in the Netherlands Brain Bank, freezing only one hemisphere, the occurrence of absence of the variants in the other hemisphere could not be tested. The similarity in clinical and pathological phenotype (i.e. severe temporal atrophy, TDP-43-positive inclusions) between the somatic *TARDBP* variant carriers and germline *TARDBP* variant carriers supports the potential pathogenicity of these variants (Caroppo *et al.*, 2016; Gonzalez-Sanchez *et al.*, 2018).

Both *TARDBP* variants identified (L41F and R42H) are located in the first exon of *TARDBP* and are non-synonymous changes predicted to impact the N-terminal domain of

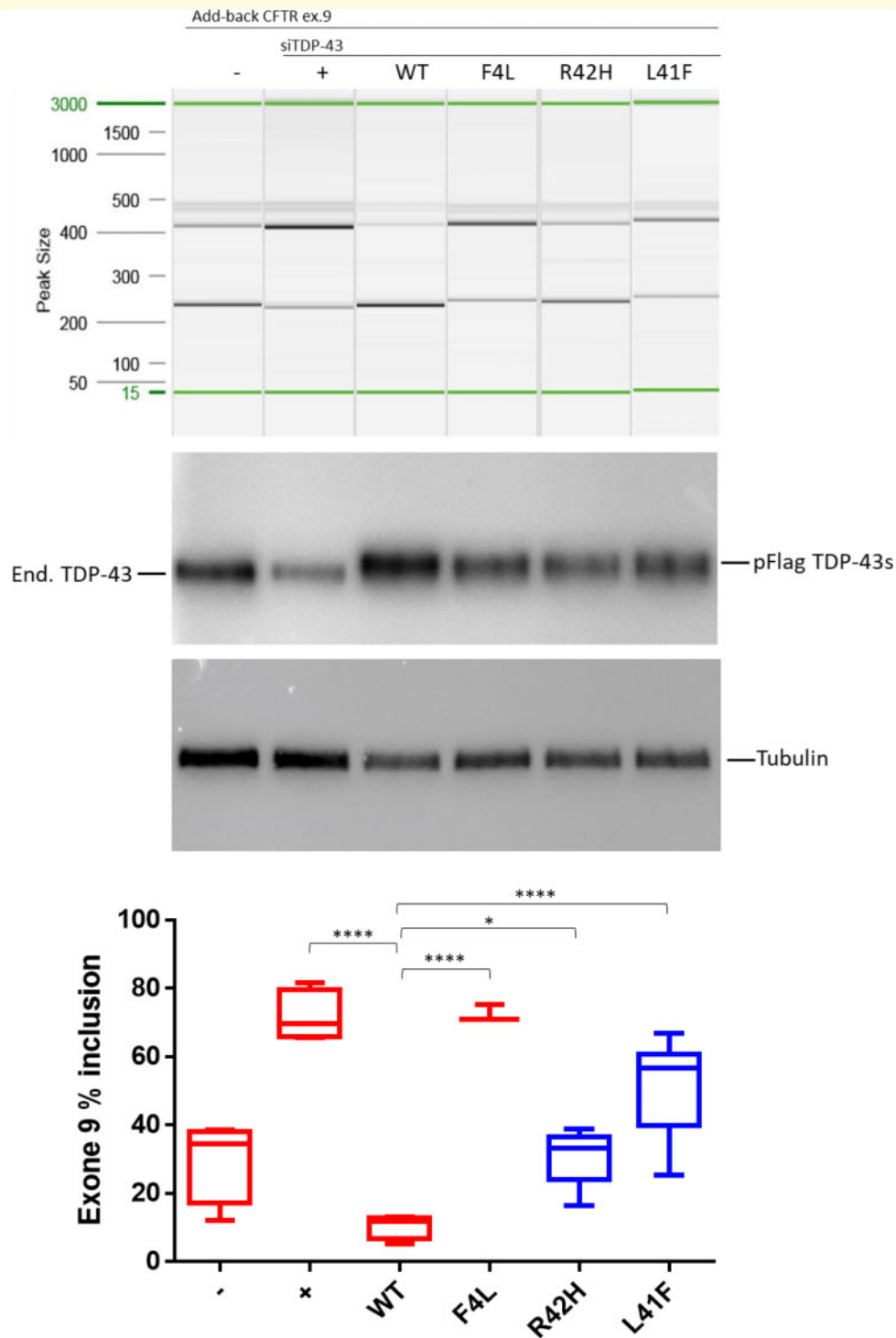


Figure 5 Impact of both *TARDBP* variants on the splicing regulation functionality of TDP-43, demonstrated by splice-in/out add-back assay of *CFTR* exon 9. From left to right: The first two lanes show the baseline measurement with both splicing in and out of exon 9 in the absence (-) or presence of TDP-43 siRNA (+). Lane 3 shows that addition of si-resistant wild-type TDP-43 can rescue the splicing functionality (WT) but this cannot be achieved by a TDP-43 carrying the F4L mutation that does not allow the protein to bind RNA (lane 4). Lanes 5 and 6 show the results obtained after the addition of mutated TDP-43 carrying the predicted damaging variants (R42H and L41F). Middle: Western blots showing equal expression of the flagged-TDP-43 wild-type and mutants (pFlag-TDP-43s) following knockdown of the endogenous protein (end. TDP-43). Tubulin was used as an internal control. Bottom: Quantification of the ratio of *CFTR* exon 9 inclusion. The standard deviation and *P*-values are reported for three independent experiments. Unpaired *t*-test was performed for statistical analysis (**P* < 0.05).

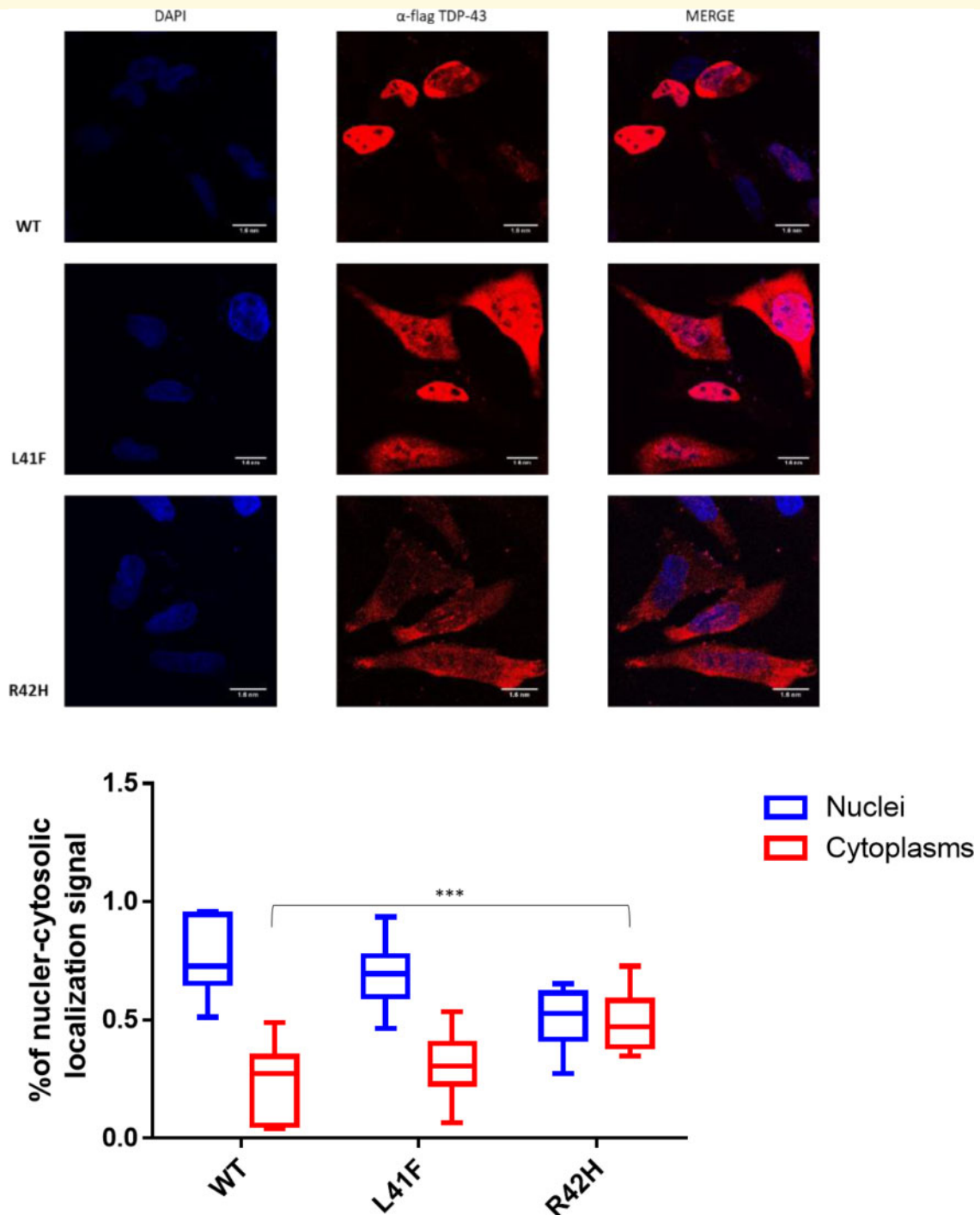


Figure 6 Impact of *TARDBP* variants on the localization of flagged-TDP-43 wild-type and mutant proteins overexpressed in HeLa cells. The overexpressed proteins were visualized using anti-Flag polyclonal antibody in a 100 nm/pixel field. Scale bar = 10 nm. *Top row*: Wild-type Flag TDP-43, followed by Flagged TDP-43s carrying both variants; L41F and R42H. *Left column*: DAPI staining to indicate the chromatin in the nucleus in blue. *Middle column*: TDP-43 stained in red with a Flag-specific antibody. *Right column*: Merged images demonstrating TDP-43 localization in the nucleus for wild-type TDP-43, whilst localizing also in the cytoplasm for both TDP43 with variant R42H and L41F. *Bottom*: Box plots showing fluorescent TDP-43 signal is quantified in the nucleus and cytoplasm for nine cells of each line. The average ratio of nuclear and cytosolic signal is plotted and compared between groups. *** $P < 0.0001$ and ** $P < 0.001$ as calculated by two-way ANOVAs between the groups illustrated.

the protein with CADD scores of 28 and 20, respectively (Chang *et al.*, 2012; Zhang *et al.*, 2013; Sasaguri *et al.*, 2016). Both variants are absent in human germline population databases ExAC and gnomAD; in fact, only eight germline variants in the first exon of *TARDBP* (amino acids 1–79) are described in the gnomAD database (120 000 participants), all extremely rare (<0.003%, 20 carriers across all eight variants combined). Our findings, identifying somatic variants in the N-terminal domain (amino acids 41 and 42) of *TARDBP*, are in contrast with all germline *TARDBP* gene variants for familial amyotrophic lateral sclerosis, and occasionally for familial FTD, reported in the glycine-rich region (GRR domain) between amino acids 262 and 414 of the TDP-43 protein (Barmada and Finkbeiner, 2010; Borroni *et al.*, 2010; Lattante *et al.*, 2013; Caroppo *et al.*, 2016; Wang *et al.*, 2016).

Our functional assays convincingly demonstrate a disruptive effect of both variants on normal *TARDBP* protein function. The impact on TDP-43 activity via *CFTR* minigene splicing was stronger for L41F than for R42H, with ~75% and 40% decrease of TDP-43 activity, respectively, compared to wild-type (D'Ambrogio *et al.*, 2009; Mompean *et al.*, 2017). Also, the redistribution of mutant TDP-43 in HeLa cells, from mostly nuclear in unaffected control to both cytoplasmic and nuclear for the R42H variants, supports the cellular pathogenicity. Together, both assays suggest that a correctly folded N-terminal domain of TDP-43 is required for nuclear localization and function, and that neurons carrying these somatic variants have dysfunctional TDP-43 and redistribution of TDP-43 protein to the cytoplasm as observed in FTD and amyotrophic lateral sclerosis brains (Chang *et al.*, 2012; Ihara *et al.*, 2013; Zhang *et al.*, 2013; Qin *et al.*, 2014; Romano *et al.*, 2015; Sasaguri *et al.*, 2016; Mompean *et al.*, 2017; Weskamp and Barmada, 2018). The resulting impact on TDP-43 function in shuttling RNA from the nucleus to the cytoplasm might lead to the protein aggregates observed in semantic dementia brains and subsequent pathogenicity for the cells and tissue in which the variants are present (Barmada and Finkbeiner, 2010; Igaz *et al.*, 2011).

It is unclear how dysfunction of a small percentage of affected neurons (2–6%, double the variant allele frequency) would lead or contribute to extensive degeneration of the temporal lobe and widespread pathology (10–15% of neurons) in the dentate gyrus. Potentially, neuronal dysfunction within one brain region can accumulate until neuron-neuron signalling is sufficiently impaired to functionally disrupt the entire region. Another consideration is that the current study considers mosaicism in bulk DNA of all neurons in the temporal lobe and/or dentate gyrus, whereas many subtypes of neurons exist in these regions, leaving the possibility that the small number of affected neurons in these patients are enriched for a specific neuronal subtype. In Alzheimer's disease, for instance, a selective loss of parvalbumin-positive GABAergic interneurons (~3% of the total neuronal population) has been observed (Brady and Mufson, 1997), and the selective dysfunction of these neurons has been causally

linked to global brain network changes and progressive amyloid pathology (Verret *et al.*, 2012; Iaccarino *et al.*, 2016; Hijazi *et al.*, 2019), indicating that small populations of affected neurons can indeed contribute to more widespread neurodegenerative processes. The challenges in interpreting selective neuronal dysfunction in the context of widespread neurodegeneration are exemplary of the overall discussion on how neurodegeneration starts and progresses (often differently between patients) throughout the brain, regardless of initial cause of the disease. Further work is needed to fully understand these processes and place the contribution of developmental and post-mitotic somatic DNA variation in the context of disrupted brain function. Cell-specific studies of semantic dementia brains carrying these somatic *TARDBP* variants may determine in which neuronal subtypes the somatic variants were present.

An important question that remains is why somatic variants were not found in all 14 brains with semantic dementia. There are several potential explanations, some of which include limitations of this study: (i) the bioinformatic filtering steps (absent in blood, CADD score > 10) may have been too stringent and removed potentially causing somatic variants; (ii) pathogenic non-coding variants may have been not detected by the present exome sequencing, and low-level copy number variants missed by the present approach; (iii) causal somatic variants may have become undetectable (disappeared) due to neuron loss in medial temporal gyrus during the neurodegenerative process; (iv) the disease may have originated from causal somatic variants that were only present in the temporal cortex or dentate gyrus opposite to the side of the examined fresh-frozen brain samples, even though we expected that somatic variants occurred prior to the hemisphere separation in brain development; and (v) multifactorial genetic or non-genetic factors may be responsible for most of the semantic dementia cases. Finally, we may have overlooked a relevant variant in the WES data by first focusing on shared variants or damaging variants in candidate genes, which may be less likely true variants. Additionally, the low-level (<0.5%) error rate of the sequencing requires stringent filtering, which may exclude variants that could be detected through panel sequencing, and further investigation of the data may uncover additional relevant variants, as was observed for the L41F variant. Pathogenicity of the remaining six variants confirmed by panel sequencing validation must be validated by future studies.

An interesting issue is whether somatic variants present in TDP-43 related genes may trigger dysregulation in the TDP-43 pathway. In analogy to this, Park *et al.* (2019) reported a significant enrichment of somatic variants in the PI3K-AKT, MAPK and AMPK pathways in Alzheimer's disease brains versus control brains. Using a KEGG pathway overrepresentation analysis, they hypothesized that multiple disease-causing somatic variants converge onto pathways that potentially affect tau phosphorylation. In our view, the next step would be to perform amplicon panel sequencing of a set of FTD-TDP related genes on both semantic dementia brains and controls in order to detect potential additional

causal somatic variants in the TDP-43 pathway. Moreover, investigating other series of semantic dementia brains may support our findings, and may give a better estimation of their frequency in semantic dementia. Finally, the present findings raise the question whether somatic variants may be causative in other types of FTD, for example somatic variants in *MAPT* causing sporadic Pick's disease. Overall, it seems warranted to carry out such targeted deep sequencing in all well-defined dementia subtypes.

Finally, although our unbiased deep sequencing approach yielded a substantial number of false-positive variants, despite extensive efforts to identify the most likely true variants, it also resulted in the detection of true-positive variants in a well-known candidate gene causative for FTD with TDP-43 pathology. In our view, future studies may choose between two alternative approaches: (i) targeted deep sequencing of bulk tissue of a large number of candidate genes in one way or another related to the pathophysiology; or (ii) single-cell whole genome sequencing generating more reliable data on true-positive variants.

In conclusion, low-level somatic pathogenic variants in the *TARDBP* gene are an underlying genetic cause of non-familial semantic dementia. This phenomenon needs investigation in other cases of semantic dementia, as well as in other early-onset neurodegenerative diseases, for example non-familial FTD with tau pathology. Moreover, in other neurodegenerative diseases, such as Alzheimer's disease or Parkinson's disease, somatic variants may also play a causal or contributing role, and deserve further investigation. Further investigation of somatic variants in known disease genes is warranted, specifically in patients without positive family history and with clearly defined focal neurodegeneration. Our findings have implications for understanding of neurodegenerative disease and the specific role of germline versus somatic variants therein. Also, negative germline variant testing might be insufficient for some diseases, and may require DNA from the appropriate tissue instead to detect somatic variants in order to determine disease causes. Finally, studying the properties of somatic disease-causing genetic variants may reveal novel underlying disease processes and point towards new therapeutic strategies.

Acknowledgements

We would like to thank the Netherlands Brain Bank and all donors that have provided the material to perform this research. Several authors of this publication are members of the European Reference Network for Rare Neurological Diseases – Project ID No 739510.

Funding

We would like to thank the funding agencies for this project; Netherlands Organization for Scientific Research (NWO) through the ZonMw Memorabel grants (project

#733050811, #733050816), the Alzheimer Nederland organization, the Gieskes-Strijbis Foundation, AriSLA (project PathensTDP) and the Beneficientia Stiftung from Lichtenstein.

Competing interests

The authors declare no competing interests.

Supplementary material

Supplementary material is available at *Brain* online

References

- Barmada SJ, Finkbeiner S. Pathogenic TARDBP mutations in amyotrophic lateral sclerosis and frontotemporal dementia: disease-associated pathways. *Rev Neurosci* 2010; 21: 251–72.
- Beck JA, Poulter M, Campbell TA, Uphill JB, Adamson G, Geddes JF, et al. Somatic and germline mosaicism in sporadic early-onset Alzheimer's disease. *Hum Mol Genet* 2004; 13: 1219–24.
- Borroni B, Archetti S, Del Bo R, Papetti A, Buratti E, Bonvicini C, et al. TARDBP mutations in frontotemporal lobar degeneration: frequency, clinical features, and disease course. *Rejuvenation Res* 2010; 13: 509–17.
- Brady DR, Mufson EJ. Parvalbumin-immunoreactive neurons in the hippocampal formation of Alzheimer's diseased brain. *Neuroscience* 1997; 80: 1113–25.
- Buratti E, Baralle FE. Characterization and functional implications of the RNA binding properties of nuclear factor TDP-43, a novel splicing regulator of CFTR exon 9. *J Biol Chem* 2001; 276: 36337–43.
- Bushman DM, Kaeser GE, Siddoway B, Westra JW, Rivera RR, Rehen SK, et al. Genomic mosaicism with increased amyloid precursor protein (APP) gene copy number in single neurons from sporadic Alzheimer's disease brains. *eLife* 2015; 4: e05116. doi: 10.7554/eLife.05116.
- Caroppo P, Camuzat A, Guillot-Noel L, Thomas-Anterion C, Couratier P, Wong TH, et al. Defining the spectrum of frontotemporal dementias associated with TARDBP mutations. *Neurol Genet* 2016; 2: e80.
- Chang CK, Wu TH, Wu CY, Chiang MH, Toh EK, Hsu YC, et al. The N-terminus of TDP-43 promotes its oligomerization and enhances DNA binding affinity. *Biochem Biophys Res Commun* 2012; 425: 219–24.
- Clarimon J, Moreno-Grau S, Cervera-Carles L, Dols-Icardo O, Sanchez-Juan P, Ruiz A. Genetic architecture of neurodegenerative dementias. *Neuropharmacology* 2020; 168: 108014.
- Coxhead J, Kurzawa-Akanbi M, Hussain R, Pyle A, Chinnery P, Hudson G. Somatic mtDNA variation is an important component of Parkinson's disease. *Neurobiol Aging* 2016; 38: 217 e1–e6.
- D'Ambrogio A, Buratti E, Stuani C, Guarnaccia C, Romano M, Ayala YM, et al. Functional mapping of the interaction between TDP-43 and hnRNP A2 in vivo. *Nucleic Acids Res* 2009; 37: 4116–26.
- Davies RR, Hodges JR, Kril JJ, Patterson K, Halliday GM, Xuereb JH. The pathological basis of semantic dementia. *Brain* 2005; 128: 1984–95.
- Ferrari R, Manzoni C, Hardy J. Genetics and molecular mechanisms of frontotemporal lobar degeneration: an update and future avenues. *Neurobiol Aging* 2019; 78: 98–110.
- Gonzalez-Sanchez M, Puertas-Martin V, Esteban-Perez J, Garcia-Redondo A, Borrego-Hernandez D, Mendez-Guerrero A, et al. TARDBP mutation associated with semantic variant primary progressive aphasia, case report and review of the literature. *Neurocase* 2018; 24: 301–5.

- Greaves CV, Rohrer JD. An update on genetic frontotemporal dementia. *J Neurol* 2019; 266: 2075–86.
- Hijazi S, Heistek TS, Scheltens P, Neumann U, Shimshek DR, Mansvelder HD, et al. Early restoration of parvalbumin interneuron activity prevents memory loss and network hyperexcitability in a mouse model of Alzheimer's disease [Internet]. *Mol Psychiatry* 2019. Available from: 10.1038/s41380-019-0483-4.
- Hodges JR, Mitchell J, Dawson K, Spillantini MG, Xuereb JH, McMonagle P, et al. Semantic dementia: demography, familial factors and survival in a consecutive series of 100 cases. *Brain* 2010; 133: 300–6.
- Hodges JR, Patterson K, Oxbury S, Funnell E. Semantic dementia. Progressive fluent aphasia with temporal lobe atrophy. *Brain* 1992; 115: 1783–806.
- Hoekstra JG, Hipp MJ, Montine TJ, Kennedy SR. Mitochondrial DNA mutations increase in early stage Alzheimer disease and are inconsistent with oxidative damage. *Ann Neurol* 2016; 80: 301–6.
- Hu WF, Chahrour MH, Walsh CA. The diverse genetic landscape of neurodevelopmental disorders. *Annu Rev Genom Hum Genet* 2014; 15: 195–213.
- Iaccarino HF, Singer AC, Martorell AJ, Rudenko A, Gao F, Gillingham TZ, et al. Gamma frequency entrainment attenuates amyloid load and modifies microglia. *Nature* 2016; 540: 230–5.
- Igaz LM, Kwong LK, Lee EB, Chen-Plotkin A, Swanson E, Unger T, et al. Dysregulation of the ALS-associated gene TDP-43 leads to neuronal death and degeneration in mice. *J Clin Invest* 2011; 121: 726–38.
- Ihara R, Matsukawa K, Nagata Y, Kunugi H, Tsuji S, Chihara T, et al. RNA binding mediates neurotoxicity in the transgenic *Drosophila* model of TDP-43 proteinopathy. *Hum Mol Genet* 2013; 22: 4474–84.
- Irish M, Addis DR, Hodges JR, Piguet O. Considering the role of semantic memory in episodic future thinking: evidence from semantic dementia. *Brain* 2012; 135: 2178–91.
- Jamuar SS, Lam AT, Kircher M, D'Gama AM, Wang J, Barry BJ, et al. Somatic mutations in cerebral cortical malformations. *N Engl J Med* 2014; 371: 733–43.
- Kim J, Kim KM, Noh JH, Yoon JH, Abdelmohsen K, Gorospe M. Long noncoding RNAs in diseases of aging. *Biochim Biophys Acta* 2016; 1859: 209–21.
- Kovacs GG, Adle-Biassette H, Milenkovic I, Cipriani S, van Scheppingen J, Aronica E. Linking pathways in the developing and aging brain with neurodegeneration. *Neuroscience* 2014; 269: 152–72.
- Kumfor F, Landin-Romero R, Devenney E, Hutchings R, Grasso R, Hodges JR, et al. On the right side? A longitudinal study of left- versus right-lateralized semantic dementia. *Brain* 2016; 139: 986–98.
- Landin-Romero R, Tan R, Hodges JR, Kumfor F. An update on semantic dementia: genetics, imaging, and pathology. *Alzheimers Res Ther* 2016; 8: 52.
- Lattante S, Rouleau GA, Kabashi E. TARDBP and FUS mutations associated with amyotrophic lateral sclerosis: summary and update. *Hum Mutat* 2013; 34: 812–26.
- Lee JH, Huynh M, Silhavy JL, Kim S, Dixon-Salazar T, Heiberg A, et al. De novo somatic mutations in components of the PI3K-AKT3-mTOR pathway cause hemimegalencephaly. *Nat Genet* 2012; 44: 941–5.
- Lee MH, Siddoway B, Kaeser GE, Segota I, Rivera R, Romanow WJ, et al. Somatic APP gene recombination in Alzheimer's disease and normal neurons. *Nature* 2018; 563: 639–45.
- Leija-Salazar M, Piette C, Proukakis C. Review: somatic mutations in neurodegeneration. *Neuropathol Appl Neurobiol* 2018; 44: 267–85.
- Leyton CE, Britton AK, Hodges JR, Halliday GM, Kril JJ. Distinctive pathological mechanisms involved in primary progressive aphasias. *Neurobiol Aging* 2016; 38: 82–92.
- Lim JS, Kim WI, Kang HC, Kim SH, Park AH, Park EK, et al. Brain somatic mutations in MTOR cause focal cortical dysplasia type II leading to intractable epilepsy. *Nat Med* 2015; 21: 395–400.
- Lin MT, Cantuti-Castelvetri I, Zheng K, Jackson KE, Tan YB, Arzberger T, et al. Somatic mitochondrial DNA mutations in early Parkinson and incidental Lewy body disease. *Ann Neurol* 2012; 71: 850–4.
- Lodato MA, Rodin RE, Bohrsen CL, Coulter ME, Barton AR, Kwon M, et al. Aging and neurodegeneration are associated with increased mutations in single human neurons. *Science* 2018; 359: 555–9.
- Lodato MA, Walsh CA. Genome aging: somatic mutation in the brain links age-related decline with disease and nominates pathogenic mechanisms. *Hum Mol Genet* 2019; 28: R197–R206.
- Lodato MA, Woodworth MB, Lee S, Evrony GD, Mehta BK, Karger A, et al. Somatic mutation in single human neurons tracks developmental and transcriptional history. *Science* 2015; 350: 94–8.
- Mackenzie IR, Neumann M. Reappraisal of TDP-43 pathology in FTLD-U subtypes. *Acta Neuropathol* 2017; 134: 79–96.
- Mackenzie IR, Neumann M, Baborie A, Sampathu DM, Du Plessis D, Jaros E, et al. A harmonized classification system for FTLD-TDP pathology. *Acta Neuropathol* 2011; 122: 111–3.
- Mesulam MM, Rogalski EJ, Wieneke C, Hurley RS, Geula C, Bigio EH, et al. Primary progressive aphasia and the evolving neurology of the language network. *Nat Rev Neurol* 2014; 10: 554–69.
- Miller ZA, Mandelli ML, Rankin KP, Henry ML, Babiak MC, Frazier DT, et al. Handedness and language learning disability differentially distribute in progressive aphasia variants. *Brain* 2013; 136: 3461–73.
- Mirzaa GM, Enyedi L, Parsons G, Collins S, Medne L, Adams C, et al. Congenital microcephaly and chorioretinopathy due to de novo heterozygous KIF11 mutations: five novel mutations and review of the literature. *Am J Med Genet A* 2014; 164A: 2879–86.
- Mokretar K, Pease D, Taanman JW, Soenmez A, Ejaz A, Lashley T, et al. Somatic copy number gains of alpha-synuclein (SNCA) in Parkinson's disease and multiple system atrophy brains. *Brain* 2018; 141: 2419–31.
- Mompean M, Romano V, Pantoja-Uceda D, Stuani C, Baralle FE, Buratti E, et al. Point mutations in the N-terminal domain of transactive response DNA-binding protein 43 kDa (TDP-43) compromise its stability, dimerization, and functions. *J Biol Chem* 2017; 292: 11992–2006.
- Mummery CJ, Patterson K, Price CJ, Ashburner J, Frackowiak RS, Hodges JR. A voxel-based morphometry study of semantic dementia: relationship between temporal lobe atrophy and semantic memory. *Ann Neurol* 2000; 47: 36–45.
- Neumann M, Mackenzie IRA. Review: neuropathology of non-tau frontotemporal lobar degeneration. *Neuropathol Appl Neurobiol* 2019; 45: 19–40.
- Nicolas G, Acuna-Hidalgo R, Keogh MJ, Quenez O, Steehouwer M, Lelieveld S, et al. Somatic variants in autosomal dominant genes are a rare cause of sporadic Alzheimer's disease. *Alzheimers Dement* 2018; 14: 1632–9.
- Palomero-Gallagher N, Zilles K. Cortical layers: cyto-, myelo-, receptor- and synaptic architecture in human cortical areas. *Neuroimage* 2019; 197: 716–41.
- Park JS, Lee J, Jung ES, Kim MH, Kim IB, Son H, et al. Brain somatic mutations observed in Alzheimer's disease associated with aging and dysregulation of tau phosphorylation. *Nat Commun* 2019; 10: 3090.
- Poduri A, Evrony GD, Cai X, Walsh CA. Somatic mutation, genomic variation, and neurological disease. *Science* 2013; 341: 1237758.
- Proukakis C, Shoaee M, Morris J, Brier T, Kara E, Sheerin UM, et al. Analysis of Parkinson's disease brain-derived DNA for alpha-synuclein coding somatic mutations. *Mov Disord* 2014; 29: 1060–4.
- Qin H, Lim LZ, Wei Y, Song J. TDP-43 N terminus encodes a novel ubiquitin-like fold and its unfolded form in equilibrium that can be shifted by binding to ssDNA. *Proc Natl Acad Sci USA* 2014; 111: 18619–24.
- Rogalski EJ, Rademaker A, Wieneke C, Bigio EH, Weintraub S, Mesulam MM. Association between the prevalence of learning

- disabilities and primary progressive aphasia. *JAMA Neurol* 2014; 71: 1576–7.
- Romano V, Quadri Z, Baralle FE, Buratti E. The structural integrity of TDP-43 N-terminus is required for efficient aggregate entrapment and consequent loss of protein function. *Prion* 2015; 9: 1–9.
- Sala Frigerio C, Lau P, Troakes C, Deramecourt V, Gele P, Van Loo P, et al. On the identification of low allele frequency mosaic mutations in the brains of Alzheimer's disease patients. *Alzheimers Dement* 2015; 11: 1265–76.
- Sasaguri H, Chew J, Xu YF, Gendron TF, Garrett A, Lee CW, et al. The extreme N-terminus of TDP-43 mediates the cytoplasmic aggregation of TDP-43 and associated toxicity in vivo. *Brain Res* 2016; 1647: 57–64.
- Seelaar H, Kamphorst W, Rosso SM, Azmani A, Masdjedi R, de Koning I, et al. Distinct genetic forms of frontotemporal dementia. *Neurology* 2008; 71: 1220–6.
- Seelaar H, Rohrer JD, Pijnenburg YA, Fox NC, van Swieten JC. Clinical, genetic and pathological heterogeneity of frontotemporal dementia: a review. *J Neurol Neurosurg Psychiatry* 2011; 82: 476–86.
- Stiles J, Jernigan TL. The basics of brain development. *Neuropsychol Rev* 2010; 20: 327–48.
- Takata A, Ionita-Laza I, Gogos JA, Xu B, Karayiorgou M. De novo synonymous mutations in regulatory elements contribute to the genetic etiology of autism and schizophrenia. *Neuron* 2016; 89: 940–7.
- van Rooij JGJ, Jhamai M, Arp PP, Nouwens SCA, Verkerk M, Hofman A, et al. Population-specific genetic variation in large sequencing data sets: why more data is still better. *Eur J Hum Genet* 2017; 25: 1173–5.
- Veltman JA, Brunner HG. De novo mutations in human genetic disease. *Nat Rev Genet* 2012; 13: 565–75.
- Verret L, Mann EO, Hang GB, Barth AM, Cobos I, Ho K, et al. Inhibitory interneuron deficit links altered network activity and cognitive dysfunction in Alzheimer model. *Cell* 2012; 149: 708–21.
- Wang W, Wang L, Lu J, Siedlak SL, Fujioka H, Liang J, et al. The inhibition of TDP-43 mitochondrial localization blocks its neuronal toxicity. *Nat Med* 2016; 22: 869–78.
- Wei W, Keogh MJ, Aryaman J, Golder Z, Kullar PJ, Wilson I, et al. Frequency and signature of somatic variants in 1461 human brain exomes. *Genet Med* 2019; 21: 904–12.
- Wiseman FK, Al-Janabi T, Hardy J, Karmiloff-Smith A, Nizetic D, Tybulewicz VL, et al. A genetic cause of Alzheimer disease: mechanistic insights from Down syndrome. *Nat Rev Neurosci* 2015; 16: 564–74.
- Weskamp K, Barmada SJ. TDP43 and RNA instability in amyotrophic lateral sclerosis. *Brain Res* 2018; 1693(Pt A): 67–74.
- Zhang YJ, Caulfield T, Xu YF, Gendron TF, Hubbard J, Stetler C, et al. The dual functions of the extreme N-terminus of TDP-43 in regulating its biological activity and inclusion formation. *Hum Mol Genet* 2013; 22: 3112–22.
- Zilles K, Palomero-Gallagher N, Amunts K. Development of cortical folding during evolution and ontogeny. *Trends Neurosci* 2013; 36: 275–84.